Modular Approach toward Supramolecular Functional Assemblies: Characterization of Donor−Spacer−Acceptor Ternary Complexes

Joe Otsuki,* Tomoko Narita, Kazuhiro Tsutsumida, Masayuki Takatsuki, and Motomu Kaneko

College of Science and Technology, Nihon University, Kanda Surugadai, Chiyoda-ku, Tokyo 101-8308, Japan

Received: February 28, 2005; In Final Form: May 7, 2005

It is shown that the noncovalent donor−spacer−acceptor (DSA) motif is useful in constructing an electron-transfer assembly. As a representative example, the equilibrium and structure of one of the DSA assemblies, consisting of Zn-tetraphenylporphyrin, a spacer unit bearing pyridine and amidinium moieties, and 3,4-dinitrobenzoic acid, were studied in detail by the extensive use of UV−vis titration, fluorescence spectroscopy, and ^{1}H NMR, with the help of a three-component equilibrium model. Complex formation and fluorescence quenching in 20 different DSA complexes constructed from a library of five donors, two spacers, and two acceptors were investigated. It has been experimentally shown that supramolecular modular approach is useful for a systematic and quick search for a functionally optimized assembly.

Introduction

The use of designed intermolecular interactions to construct supramolecular donor (D)−acceptor (A) assemblies, in which photoinduced electron transfer takes place, has been receiving considerable attention, since this approach has significant advantages over the covalent counterparts for the construction of complex multicomponent structures.[1,2] The majority of noncovalent DA pairs thus far reported involve specifically modified donor and acceptor molecules in a way that they self-assemble into a supramolecular binary complex or dyad. One of the rare motifs of chromophore assembly is ternary complex system in which a donor and an acceptor is held together by a spacer (S) unit.[3] The use of an independent spacer molecule having two recognition sites, which can bind both donor and acceptor molecules to form a ternary complex, DSA, merits special attention, since this modular approach would allow one to optimize each component independently, keeping the other part unaffected. Thus, it should be suitable to survey a combinatorial library of DSA systems to find an optimized structure for, say, efficient electron transfer. In addition, the ternary system mimics more closely the reaction center of photosynthesis where chromophores are precisely disposed by the interactions with the matrix proteins rather than by direct chromophore−chromophore interactions.

We have previously reported a ternary complex wherein Zn-tetraphenylporphyrin (**D1**) and 3,4-dinitrobenzoic acid (**A1**) are held together by a spacer molecule (**S1**), which is a pyridine derivative with an amidine moiety. This spacer holds **D1** and **A1** together through axial coordination and amidinium−carboxylate salt bridge interactions, respectively.[4] In this ternary complex, **D1S1A1**, in CH_2Cl_2, the fluorescence of the Zn-porphyrin is nearly completely quenched by the electron acceptor as confirmed by the steady-state fluorescence measurements. The picosecond time-resolved fluorescence lifetime measurements suggested a very fast quenching (<20 ps). It was also found that the quenching of the triplet excited state is facilitated by the ternary complex formation. Energetic considerations suggested that the quenching is due to the intracomplex electron transfer. Although the efficacy of the quenching of the singlet and triplet excited states has thus been established, detailed analysis of the ternary complex formation has not been reported yet. The argument that the modular approach can produce a variety of DSA systems has not been proved experimentally either.

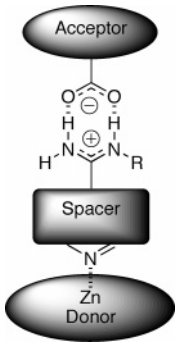

Figure 1. Modular approach to construct DSA ternary complexes, using a spacer that binds both to a donor and an acceptor via axial coordination and amidinium−carboxylate salt bridge interactions, respectively.

Herein, we wish to report a detailed analysis of the equilibrium among the three components by the use of UV−vis titration and a model of three-component equilibrium. Also, a library of DSA systems has been actually constructed from components, showing that the supramolecular modular approach is indeed useful in optimizing a specific part, keeping other parts unchanged, and producing various DSA systems readily. Axial coordination[2] and amidinium−carboxylate salt bridge interactions[5,6] are used throughout for the connections in DS and SA, respectively, as shown in Figure 1. The molecular components used in this study are displayed in Chart 1.

Results and Discussion

Interaction between S1 and A1. We have established the formation of the ternary complex, **D1S1A1**, in which an efficient

* Author to whom correspondence should be addressed. E-mail: otsuki@chem.cst.nihon-u.ac.jp.

10.1021/jp051012f CCC: $30.25
Published on Web 06/18/2005

CHART 1: Components for DSA Complexes

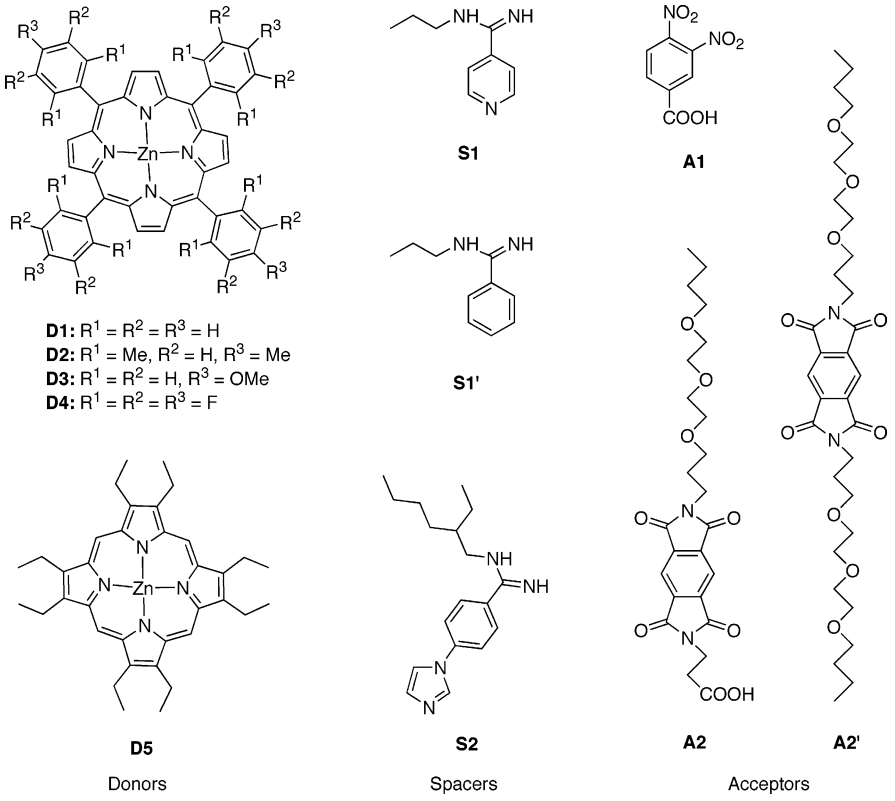

electron transfer from the photoexcited **D1** to the acceptor through the spacer was suggested.[4] However, the detailed analysis of the equilibrium reaction is yet to be presented. In going from binary DA systems to ternary DSA systems, several new issues should be addressed. One has to ensure that the interactions between the donor and spacer and those between the spacer and acceptor must be orthogonal to exclude the formation of unwanted assemblies such as DSD or ASA. Also, a direct interaction between the donor and acceptor must be avoided. We have carefully analyzed the formation of the ternary complex, **D1S1A1**, as a representative example. We start with the analysis of the association between **S1** and **A1** and then describe the association between **D1** and **S1**, followed by the detailed analysis of the ternary **D1S1A1** complex formation.

Figure 2 shows the variations of chemical shifts of protons in **A1** in a ^{1}H NMR titration experiment wherein incremental amounts of **S1** (0−8 mM) were added to a CD_2Cl_2 solution of **A1** (4 mM). All protons experienced upfield shifts in proportion to the amount of added **S1** until the equivalent amount was reached, when the shifts leveled off with more **S1** at about $\Delta\delta = 0.1$ ppm. This shows that the association constant between **S1** and **A1** is beyond the range that can be determined by the ^{1}H NMR method ($\gg 10^3$ M^{-1}). This is consistent with the strong binding of the amidinium−carboxylate salt bridge, which is a double hydrogen bonding with favorable secondary interactions further augmented by the electrostatic force.[5,6]

Interaction between D1 and S1. Axial coordination to Zn-porphyrins is most conveniently measured by means of electronic absorption spectroscopy, since axial coordination is accompanied by a red-shift in the Q- and Soret-band peaks by ∼15 nm.[7] The visible spectra were recorded following the addition of incremental amounts of **S1** into a CH_2Cl_2 solution of **D1** (10 μM) as in Figure 3. It is clear from the red-shift by 15−20 nm with isosbestic points that a 1:1 adduct is formed through axial coordination. The decrease in the absorbance at the original λ_{max} at 548 nm is thus a quantitative measure of complex formation. By using the data extracted as a function of added spacer concentration, the association constant between **D1** and **S1** was determined as $K_{D1S1} = 8.1 \times 10^3$ M^{-1} (CH_2Cl_2, 25 °C), by means of a least-squares procedure.[8]

The association constant is on the same order of magnitude with that for the coordination of pyridine to **D1**.[9] However, even when **S1′**, which lacks a pyridine moiety, was added, the Q-band changed in a way similar to the case of **S1**, indicating the occurrence of axial coordination. The association constant in this case was obtained as $K_{D1S1'} = 6.5 \times 10^3$ M^{-1}. This proves that the amidine group can interact with Zn-porphyrins as well. This in turn suggests that, in complex **D1S1**, the pyridine and amidine groups could compete with one another for the binding to the Zn ion in porphyrin.

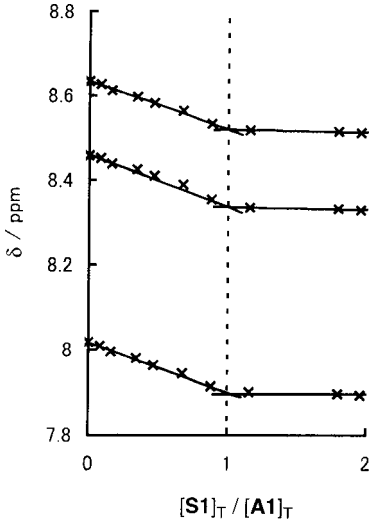

Figure 2. ^{1}H NMR titration of **A1** (4 mM) with **S1** (0−8 mM) in CD_2Cl_2.

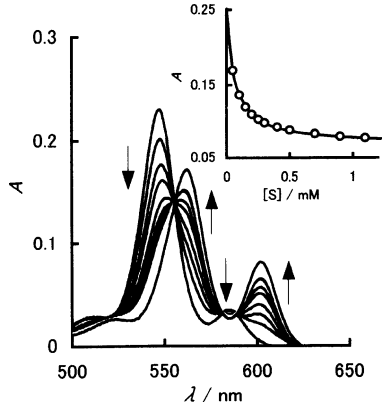

Figure 3. Spectral changes in the Q-band region of **D1** (10 μM) upon addition of **S1** (0−1.2 mM) in CH_2Cl_2 at 25 °C. Inset: Changes in absorbance at 548 nm. Observed values (circles) are curve-fitted (line) to obtain the association constant.

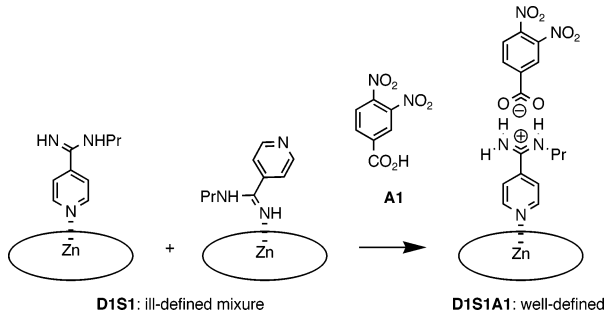

Figure 4. A "correction" mechanism to yield the right final structure.

^{1}H NMR is another powerful method for the investigation of axial coordination, owing to the large ring-current effect exerted by the porphyrin macrocycle.[10] The values of upfield shift for the protons ortho and meta to the pyridine-*N* in **S1** upon the addition of **D1** (10 mM) to **S1** (10 mM) in CD_2Cl_2 were 3.0 and 0.9 ppm, respectively. These values are too small for a pyridine moiety axially bound to **D1** through the pyridine-*N*;[11] the upfield shifts for ortho and meta protons in pyridine axially coordinating to **D1** are 5.9 and 1.8 ppm, respcetively.[10b] This supports the picture that not only the pyridine-*N* but also the amidine-*N*'s are interacting axially with the Zn ion in **D1**. This could be undesirable from the viewpoint of constructing a well-defined supramolecular structure.

This ambiguity of structural programming in the **D1S1** assembly is resolved by a "correction" process by adding **A1** in the present case. The **D1**-induced upfield shifts for the protons ortho and meta to the pyridine-*N* in **S1** in ternary complex **D1S1A1** are 6.06 and 1.79 ppm,[4] consistent with an exclusive axial coordination through the pyridine-*N*. This correction process is schematically illustrated in Figure 4. Both of the pyridine-*N* and amidine-*N*'s in **S1** are capable of coordinating to **D1**; the structure of **D1S1** is not well-defined. However, **A1** selectively occupies the amidine site because of the strong amidinium−carboxylate interaction, leaving the pyridine-*N* as the only site that can bind to **D1**. The exclusive formation of the well-defined DSA complex is assured in this way.

Equilibrium among D1, S1, and A1. The ternary complex formation was followed by UV−vis spectroscopy for a CH_2Cl_2 solution containing **D1** (10 μM), **S1** (1.5 mM), and increasing amounts of **A1**. The change in absorbance at 548 nm upon the addition of **A1** is shown in Figure 5a. Qualitatively, the larger absorbance at this wavelength indicates that more **D1** is present without an axial ligand, see Figure 3. The amount of complexed **D1** is only slightly affected by low concentrations of **A1** (<0.5 mM) Then, the axial ligand starts to detach significantly upon the addition of more than ~0.5 mM **A1** until the amount of free **D1** reaches a constant value when more than 1.5 mM **A1** is present.

Since a three-component equilibrium has never been analyzed quantitatively, in contrast to the conventional two-component DA systems,[2] a model for the three-component equilibrium has been developed, especially to explain the sigmoidal behavior

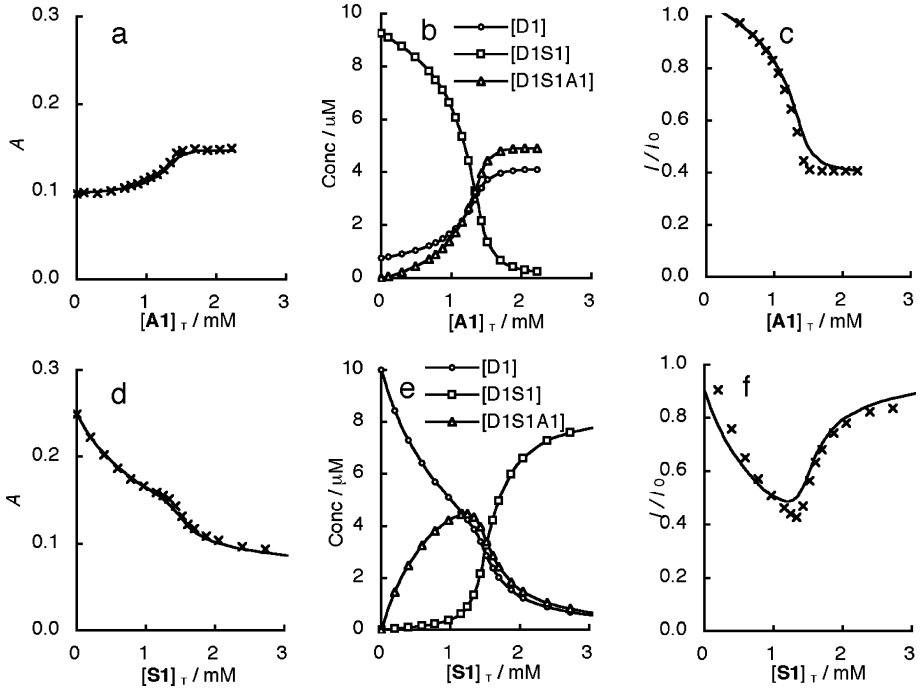

Figure 5. Titration experiments in CH_2Cl_2 at 25 °C. Crosses are observed values, while lines and the other marks are calculated results. Upper panels: **A1** was added to a mixture of **D1** (10 μM) and **S1** (1.5 mM). (a) Absorbances at 548 nm. (b) Calculated concentration profiles. (c) Fluorescence intensities (λ_{ex} = 556 nm). Lower panels: **S1** was added to a mixture of **D1** (10 μM) and **A1** (1.5 mM). (d) Absorbances at 548 nm. (e) Calculated concentration profiles. (f) Fluorescence intensities (λ_{ex} = 556 nm).

mentioned above. The equilibrium is represented by eqs 1−3 for self-assembled ternary DSA systems.

$$D + S \rightleftharpoons DS \qquad K_{DS} = [DS]/[D][S] \qquad (1)$$

$$S + A \rightleftharpoons SA \qquad K_{SA} = [SA]/[S][A] \qquad (2)$$

$$D + S + A \rightleftharpoons DSA \qquad K_{DSA} = [DSA]/[D][S][A] \qquad (3)$$

In this model, it is assumed that S can bind both to D and A, while there is no direct interaction between D and A. By introducing an approximation that the concentration of D is much smaller than those of S and A, as appropriate for the present system, the concentrations of all species present in solution can be expressed with the three association constants, K_{DS}, K_{SA}, and K_{DSA}. The full mathematical derivation is given in Supporting Information. The value of K_{DS} is obtained from the UV−vis binding study between D and S. Then, the values of K_{SA} and K_{DSA} are unknown parameters to be simultaneously determined from the ternary binding study. For the case of **D1**, **S1**, and **A1**, a value of $K_{D1S1} = 8.1 \times 10^3\ M^{-1}$ was obtained by a titration experiment as shown in Figure 3. Then, the best-fitting curve in the three-component titration as shown in Figure 5a gave values of $K_{S1A1} = 2.2 \times 10^5\ M^{-1}$ and $K_{D1S1A1} = 1.9 \times 10^8\ M^{-2}$. Now that all the relevant association constants are known, concentration profiles can be calculated. The concentrations of **D1**, **D1S1**, and **D1S1A1** are plotted as the functions of added **A1**, as shown in Figure 5b. It is now clear that the sigmoidal increase of **D1** and **D1S1A1** at the expense of **D1S1** is the reason of the sigmoidal absorbance change.

When the binding strengths in DS and SA are independent, it is shown that $K_{DS}K_{SA} = K_{DSA}$. Any deviation from this relationship indicates the presence of a cooperativity in the two binding events. If $K_{DS}K_{SA} > K_{DSA}$, then the binding is negatively cooperative, while if $K_{DS}K_{SA} < K_{DSA}$, then the binding is positively cooperative. In this particular case of **D1S1A1**, the former relation holds, indicating that there is a negative cooperativity. Two reasons may be invoked as to why the presence of **A1** reduces the binding of **S1** with **D1**. One is that **A1** occupies the amidine group in **S1**, allowing only the pyridine-*N* to bind to **D1** (vide supra). The other is that the amidinium−carboxylate salt bridge formation produces a positive charge in **S1**, which may reduce the affinity of the pyridine-*N* toward **D1**.

Fluorescence intensities during this titration are shown in Figure 5c. A sigmoidal behavior is also observed. Since the amount of each porphyrin species is known, the relative fluorescence intensities from ternary complex **D1S1A1** (Φ_{DSA}) can be obtained by curve-fitting to the data (see Supporting Information). Figure 5c includes the curve thus obtained by using $\Phi_{D1S1A1} = 0.0$, indicating a near-unity efficiency of quenching in the ternary complex, which we attribute to the intracomplex electron transfer.[4]

Fully reversible nature of this process is demonstrated by an addition experiment with a different sequence, that is, a solution of **D1** (10 μM) and **A1** (1.5 mM) was titrated with **S1**, the result of which is shown in Figure 5d. In this case, the absorbance decreased with increasing **S1** concentration with a bump around 1.2 mM of added **S1**. Exactly the same set of parameters (K_{D1S1}, K_{S1A1}, and K_{D1S1A1}) as obtained above nicely reproduced the observed change, as shown by the curve superimposed on the graph. The concentration profiles for each species revealed that the bump corresponds to the concentration at which the amount of **D1S1A1** passes through the maximum (Figure 5e). Fluorescence intensity in this case passes through the minimum at around 1.2 mM of added **S1**, which corresponds to the point where the maximum amount of **D1S1A1** is present (Figure 5f). The calculated fluorescence curve is obtained by using $\Phi_{D1S1A1} = 0.0$, again fitting reasonably well with the observed values.

TABLE 1: Properties of Donors and Their Interactions with Spacers and Acceptors

D	$E^{+/0}$/V[a]	E_{00} [b]/ eV	K_{DS1} [c]/ $10^3\ M^{-1}$	K_{DS2} [c]/ $10^3\ M^{-1}$	ΔG_{A1} [d]/ eV	ΔG_{A2} [d]/ eV
D1	0.37[e]	2.06	8.1	12.1	−0.50	−0.35
D2	0.61[e]	2.06	26.0	4.6	−0.26	−0.11
D3	0.27[f]	2.05	6.6	26.5	−0.59	−0.44
D4	0.83[g]	2.15	133.1	40.8	−0.13	0.02
D5	0.21[h]	2.17	1.5	1.3	−0.77	−0.62

[a] The first oxidation potentials versus ferrocenium/ferrocene in CH_2Cl_2. [b] Singlet-state energies obtained from the lowest energy λ_{max} for axially coordinated Zn-porphyrins. [c] Values in CH_2Cl_2 at 25 °C. Conditional standard deviations are less than 7%. [d] Gibbs free energy changes upon electron transfer from $^1D^*$ to form ($D^{\bullet+} + A^{\bullet-}$). [e] Reference 12. [f] Reference 13. [g] Reference 14. [h] A value reported versus saturated calomel electrode[15] was converted by subtracting 0.42 V to give the value versus ferrocenium/ferrocene.[16]

Some New Entries for the Modular Approach. One of the advantages of the modular approach is that each component can be readily replaced by a different molecule which is specifically optimized independently, keeping the other part unaltered. Another, but related, advantage is that different combinations can produce a library of DSA structures, just by mixing components. For example, for a three-component system such as the one in the present case, the preparation of *l* donors, *m* spacers, and *n* acceptors would produce a total of *lmn* final ternary DSA structures. To demonstrate these concepts experimentally, we have used some more porphyrin derivatives, **D2**−**D5**, and added a new spacer, **S2**, and a new acceptor, **A2**, as components for the ternary complex. Before discussing a DSA library, we will describe the properties of these new entries as components for the library.

A total of five porphyrins were chosen as donors. Four of them are based on Zn-*meso*-tetraphenylporphyrin (**D1**) with variously substituted phenyl groups, such as sterically demanding mesityl groups (**D2**), electron-donating methoxyphenyl groups (**D3**), and electron-withdrawing pentafluorophenyl groups (**D4**). The other porphyrin used is Zn-β-octaethylporphyrin (**D5**). Relevant photophysical properties of these porphyrins, that is, the first oxidation potentials ($E^{+/0}$) and the singlet-state energies (E_{00}), are listed in Table 1.

As a new entry into the spacer family, we prepared **S2**, which has an imidazole moiety. The imidazole moiety was chosen as a binding site to Zn-porphyrin, because it is known that imidazole derivatives coordinate more strongly to Zn-porphyrins than pyridine derivatives do.[17−19] The binding between porphyrins **D1**−**D5** and spacers **S1** and **S2**, investigated by means of UV−vis titration, is also summarized in Table 1. Although the association data show that **S2** can be either a stronger or a weaker ligand than **S1** depending on the structure of porphyrin, these comparisons are not specifically for pyridine versus imidazole functions, since these spacer molecules could bind to Zn-porphyrins through their amidine group as well, as described earlier.

The structure of a ternary complex involving **S2** was firmly established by ^1H NMR titration. ^1H NMR spectra were recorded as portions of **D1** were added to a 1:1 solution of **S2** and **A1** in $CDCl_3$, as shown in Figure 6. All protons experienced upfield shifts upon addition of **D1**. Especially large changes were induced for protons on the imidazole ring in **S2**. As the distance from the imine-*N* in the imidazole ring increases, the magnitude

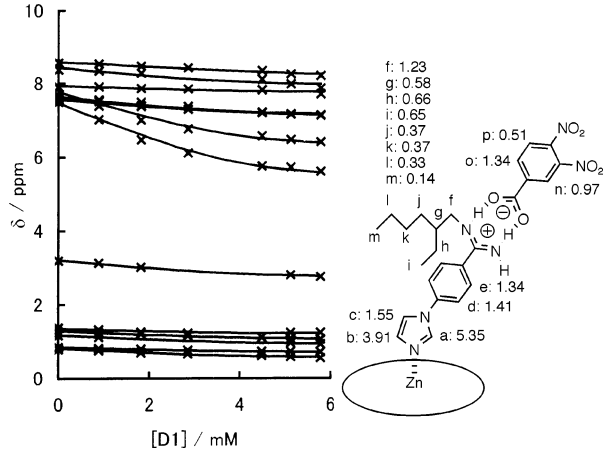

Figure 6. Changes in chemical shifts of protons in **S2** (4 mM) and **A1** (4 mM) upon the addition of **D1** in $CDCl_3$.

of the shift decreases, in accord with axial coordination via the imine-*N* in the imidazole ring.[10] A least-squares curve-fitting procedure[8] gave an association constant of $K_{D1(S2A1)}$ ($=K_{D1S2A1}/K_{S2A1}$) $= 3.4 \times 10^3$ M^{-1} for the equilibrium, assuming that all **S2** and **A1** are bound in the form of **S2A1** in these conditions. The values extrapolated to the infinite amount of **D1** according to the isotherms correspond to the limiting values of the chemical shift changes, which are shown on the chemical structure in Figure 6.

Pyromellitic diimide is a well-known acceptor for the excited electron from Zn-porphyrins.[19b,20−22] The acceptor, **A2**, was designed to have a carboxyl moiety for the binding with a spacer and an oligoether moiety as a solubilizing group. This acceptor quenches the fluorescence of **D1** only slightly through a bimolecular process without a spacer ($K_{SV} = 59$ M^{-1}), while it quenches the fluorescence of **D1** more efficiently when a spacer is present. For example, the fluorescence of **D1** diminishes by about 40% by **A2** (2 mM) in the presence of **S1** (1.2 mM). In addition, the use of **A2′**, without a carboxyl group, in place of **A2**, caused little quenching even in the presence of **S1**, providing evidence that a carboxyl group is required in forming the ternary electron-transfer assembly.

Included in Table 1 are approximate Gibbs free energy changes associated with electron transfer from the singlet excited state of porphyrin to acceptors. The listed values are calculated according to $\Delta G = E^{+/0} - E_{00} - E_A^{0/-1}$, using the reduction potentials ($E_A^{0/-1}$) of **A1** in the salt bridge form (−1.19 V[4]) and **A2** (−1.34 V[22b]). The negative free-energy values point to the feasibility of electron-transfer reactions in these assemblies, except for one case (i.e., **D4**/**A2**). These values are only approximate, however, since the Coulomb interaction term in the charge-separated state is neglected and it is known that the oxidation potential is slightly affected by axial ligation for some porphyrins.[12,22]

Modular Approach: Combinatorial Library of DSA Ternary Complexes. We have prepared a DSA library from five donors (**D1**−**D5**), two spacers, and two acceptors (**A1** and **A2**) ($l = 5$, $m = 2$, $n = 2$). The total of 20 DSA structures were obtained from these nine components. Furthermore, 20 model systems, which lack either a spacer or an acceptor, were also obtained quite readily. Porphyrin solutions (10 μM) in CH_2Cl_2 containing either one or both a spacer (1 mM) and an acceptor (4 mM) were prepared, and UV−vis and fluorescence spectra were measured. From the absorption spectra, the amounts of Zn-porphyrin complexed with an axial ligand can be known, which are arranged in Figure 7a. The absorption spectra only concern

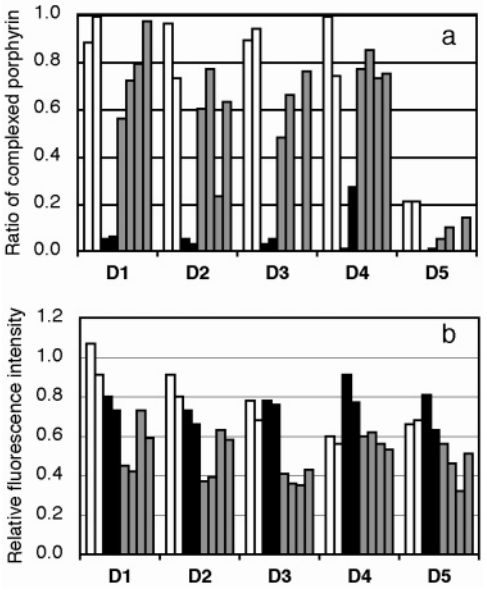

Figure 7. Binding to porphyrins and fluorescence quenching by spacers and acceptors: [**D**] = 10 μM, [**S**] = 1 mM, and [**A**] = 4 mM, CH_2Cl_2, 25 °C.[23] Eight columns for each porphyrin correspond to, from left to right, **S1**, **S2**, **A1**, **A2**, **S1A1**, **S1A2**, **S2A1**, and **S2A2**. Thus, white, black, and gray columns indicate that only a spacer, only an acceptor, and both a spacer and an acceptor are present, respectively. (a) The ratios of complexed porphyrins (DS and DSA) to the total porphyrin species. (b) Fluorescence intensities relative to a pure porphyrin solution ($\lambda_{ex} = 556$ nm).

the binding of D and S and give no information as to the binding of S and A. However, if it is assumed that the latter association is stong enough to a near completion, which may be justified under the experimental conditions, the absorption spectra are considered as indicators for the ternary complex formation.

From the inspection of Figure 7a, it is apparent that more than ∼80% of Zn-porphyrins are complexed in the presence of a 1 mM spacer (white columns), except for **D5**, for which the absorption spectra indicate only about 20% is complexed. In sharp contrast, acceptors by themselves barely interact with Zn-porphyrins, except for the combination of **D4** and **A2**. There is a trend that the mixture of spacer and acceptor bind to Zn-porphyrin less than spacer alone (compare white and gray columns).

As for the fluorescence intensities displayed in Figure 7b, it can be seen for **D1**, **D2**, and **D3** that neither a spacer nor an acceptor alone quenches the porphyrin fluorescence significantly. This is because spacers are not electron acceptors, although they interact with porphyrins, while acceptors only quench a small portion of porphyrin fluorescence, since they are not bound to the porphyrin. The presence of both a spacer and an acceptor is required to effect an efficient quenching (gray). For **D1** and **D2**, **S1** is a better spacer than **S2** in facilitating fluorescence quenching, while for **D3**, both of them work comparatively (compare the left two and the right two gray columns). For **D4**, a significant quenching is caused by the spacers, and further addition of acceptors does not further reduce the fluorescence intensity. Thus, the reason of the quenching in the case of **D4** may not be reductive electron transfer as assumed for other porphyrins. The free-energy changes accompanying the electron transfer involving **D4** are very small or even positive as shown in Table 1. Finally, a clear trend is not observed for **D5**. The quenching may not involve a complex, since axial coordination is not observed for **D5** anyway. The free-energy gains for possible electron transfer are

large as shown in Table 1, and therefore, the quenching may be due to fast bimolecular processes.

For the present system, a desirable combination of components is such that a ternary complex is formed as much as possible and the porphyrin fluorescence is quenched as much as possible. Among the library under survey, it is for the combinations of **D1S1A2**, **D2S1A2**, and **D3S2A2** that more than 70% of porphyrin molecules are complexed and the fluorescence intensity is reduced down to ∼40%. Thus, the modular supramolecular approach allows us to survey a large number of combinations systematically to search for an optimized structure for desired functions in a quick and economical way.

Conclusion

We have constructed donor−spacer−acceptor (DSA) ternary complexes from various components, with applications to photoinduced electron-transfer model systems in mind. The equilibrium among the three component was analyzed in detail for a combination of Zn-porphyrin (**D1**), a spacer (**S1**), and 3,4-dinitrobenzoic acid (**A1**). A three-component equilibrium model was developed to explain the observed association behavior. A new spacer and a new acceptor were introduced in addition to previously reported components. Then, it has been experimentally shown that a large number of DSA systems can be obtained from the combinations of components, showing the usefulness of supramolecular modular approach. The modular approach would be applicable to other functional supramolecular systems. It is an economical approach to produce a vast array of supramolecular complexes, well-suited to search for an optimum structure in a systematic but quick way.

Experimental Section

Instruments. ^{1}H NMR spectra were recorded on a JEOL JNM-GX400 spectrometer. EIMS spectra were taken with a Shimazdu GCMS-QP5050A spectrometer equipped with a direct injection unit. FABMS measurements were done by I. Yoshikawa of the University of Tokyo. Elemental analyses were performed by the Chemical Analysis Center of the College of Science and Technology, Nihon University. UV−vis and fluorescence data were obtained using Shimadzu UV-2400PC and RF-5300PC spectrophotometers, respectively. EI-HRMS measurements were carried out by the Chemical Analysis Center of the College of Pharmacy, Nihon University.

UV−Vis and Fluorescence Measurements. All measurements were carried out in spectroscopic grade CH_2Cl_2 themostatted at 25 °C. Solutions containing 10 μM porphyrin were prepared on the basis of reported molar absorption coefficients at a Q-band peak (**D1**,[24] **D2**,[25] **D3**,[24] **D4**,[26] and **D5**[24]). Association constants between porphyrins and spacers (K_{DS}) were obtained by titration of porphyrin solutions by acceptors along with a least-squares curve-fitting procedure.[4] The conditional standard deviations were within ±7%. Other association constants (K_{DS} and K_{DSA}) were obtained as described in the text and in the Supporting Information. The ratios of complexed porphyrins in Figure 7a were determined by using the spectral data for ligated and free Zn-porphyrins obtained by the above-mentioned titration experiments. The ratio of absorbances at two different wavelengths was used in this determination to cancel out a small dilution effect caused by the addition of solutions. Relative fluorescence intensities (I/I_0) were obtained by integrating over the whole range of emission in wavenumbers and were normalized with respect to the Zn-porphyrin fluorescence (I_0).

Materials. Porphyrins **D1** (low chlorin) and **D5** were commercial and were used as received. Porphyrins **D2**, **D3**, and **D4** were prepared by inserting a Zn ion into the free-base precursors according to a literature method.[27] Spacers, **S1** and **S1′**, were obtained as in a previous report.[4]

3-(2-(2-Butoxyethoxy)ethoxy)propylamine. This compound was prepared by reducing 3-(2-(2-butoxyethoxy)ethoxy)propylnitrile according to a literature procedure[28] except that the reaction was achieved with 30-atom H_2 in an autoclave.

A2′. A solution of 3-(2-(2-butoxyethoxy)ethoxy)propylamine (216 mg, 1.0 mmol) and pyromellitic dianhydride (87 mg, 0.40 mmol) in DMF (30 mL) was heated at 70 °C for 1.5 h and then refluxed for 21 h under Ar. The solvent was evaporated and the residue was chromatographed over silica gel with $CHCl_3$/MeOH (4/1) as eluent to afford an off-white solid (143 mg, 58%), mp 69−73 °C. ^{1}H NMR (CD_3OD): δ 0.91 (6H, t, J = 7.0 Hz), 1.34 (4H, sextet, J = 7.0 Hz), 1.51 (4H, quintet, J = 7.0 Hz), 1.96 (4H, quintet, J = 7.0 Hz), 3.42−3.56 (24H), 3.83 (4H, t, J = 7.0 Hz), 8.21 (2H, s). EIMS: m/z = 620 (M^+). Anal. Found: C, 61.30; H, 7.61; N, 4.64%. Calcd for $C_{32}H_{48}N_2O_{10}\cdot 1/2(H_2O)$: C, 61.03; H, 7.84; N, 4.45%.

A2. A solution of pyromellitic dianhydride (792 mg, 3.63 mmol) in DMF (100 mL) was dropwise added to a stirred solution of 3-(2-(2-butoxyethoxy)ethoxy)propylamine (798 mg, 3.64 mmol) and β-alanine (325 mg, 3.65 mmol) in DMF (40 mL). The solution was heated at 70 °C for 1.5 h and then was refluxed for 23 h. The solvent was evaporated to give a yellow solid to which MeOH was added. The mixture was filtered, and the filtrate was evaporated. The obtained solid, after being washed with hexane, was chromatographed over silica gel twice (CH_2Cl_2/MeOH (100/1) and $CHCl_3$/MeOH (10/1)) and then was treated with activated charcoal to afford a white powder (177 mg, 10%), mp 157−161 °C. ^{1}H NMR (CD_3OD): δ 0.91 (3H, t, J = 7.0 Hz), 1.31 (2H, sextet, J = 7.0 Hz), 1.50 (2H, quintet, J = 7.0 Hz), 1.95 (2H, quintet, J = 7.0 Hz), 2.63 (2H, t, J = 7.2 Hz), 3.42−3.56 (12H), 3.83 (2H, t, J = 7.0 Hz), 3.97 (2H, t, J = 7.2 Hz), 8.21 (2H, s). EIMS: m/z = 490 (M^+). Anal. Found: C, 58.60; H, 6.13; N, 5.47%. Calcd for $C_{24}H_{30}N_2O_9$: C, 58.77; H, 6.16; N, 5.71%.

S2. Hydrogen chloride was bubbled into a solution of 4-(1-imidazol)benzonitrile[29] (600 mg, 3.6 mmol) and EtOH (distilled over CaO and Mg; 0.30 mL, 3.6 mmol) in $CHCl_3$ (distilled over CaH_2, 5 mL), and the solution was stirred at 0 °C for 18 h. The solution was poured into aqueous NaOH and was extracted with $CHCl_3$, which was then dried over $MgSO_4$. The evaporation of the solvent gave the iminoether as a white solid (232 mg). To the solid was added a solution of 2-ethylhexylamine hydrochloride (232 mg, 1.4 mmol) in EtOH (8 mL), and the solution was refluxed under N_2 for 4 h. The yellow oily material obtained upon evaporation of the solvent was chromatographed on alumina, being eluted with CH_2Cl_2/MeOH (9/1), to give the hydrochloride salt of **S2** as a yellow solid. This was treated with aqueous NaOH and was extracted into $CHCl_3$, which was then dried over $MgSO_4$. The evaporation of the solvent afforded neutral **S2** as an oil (180 mg, 43%). ^{1}H NMR (CD_3OD) δ 0.97−0.87 (6H, m), 1.29−1.50 (8H, m), 1.72 (1H, m), 3.20 (2H, d, J = 6.8 Hz), 7.17 (1H, t, J = 1.2 Hz), 7.65 (1H, t, J = 1.2 Hz), 7.69 (2H, d, J = 8.8 Hz), 7.81 (2H, d, J = 8.8 Hz), 8.23 (1H, t, J = 1.2 Hz). FABMS: m/z = 299 (MH^+). EI−HRMS: found, 298.2167; calcd for $C_8H_{26}N_4$, 298.2157.

Acknowledgment. This work was supported by grants from Japan Ministry of Education, Science, Technology, Culture, and Sports, Saneyoshi Scholarship Foundation, Tokyo Ohka Foundation for the Promotion of Science and Technology, and Nihon University. We thank I. Yoshikawa of the University of Tokyo for FABMS measurements.

Supporting Information Available: Mathematical treatment of the three-component equilibrium. This material is available free of charge via the Internet at http://pubs.acs.org.

References and Notes

(1) For reviews, see: (a) El-Khouly, M. E.; Ito, O.; Smith, P. M.; D'Souza, F. *J. Photochem. Photobiol., C* **2004**, *5*, 79−104. (b) Blanco, M.-J.; Jiménez, M. C.; Chambron, J.-C.; Heitz, V.; Linke, M.; Sauvage, J.-P. *Chem. Soc. Rev.* **1999**, *28*, 293−305. (c) Piotrowiak, P. *Chem. Soc. Rev.* **1999**, *28*, 143−150. (d) Hayashi, T.; Ogoshi, H. *Chem. Soc. Rev.* **1997**, *26*, 355−364. (e) Ward, M. D. *Chem. Soc. Rev.* **1997**, *26*, 365−376.

(2) Otsuki, J. *Trends Phys. Chem.* **2001**, *8*, 61−72.

(3) Hunter C. A.; Shannon, R. J. *Chem. Commun.* **1996**, 1361−1362.

(4) Otsuki, J.; Takatsuki, M.; Kaneko, M.; Miwa, H.; Takido, T.; Seno, M.; Okamoto, K.; Imahori, H.; Fujitsuka, M.; Araki, Y.; Ito, O.; Fukuzumi, S. *J. Phys. Chem. A* **2003**, *107*, 379−385.

(5) Fitzmaurice, R. J.; Kyne, G. M.; Douheret, D.; Kilburn, J. D. *J. Chem. Soc., Perkin Trans. 1* **2002**, 841−864.

(6) (a) Roberts, J. A.; Kirby, J. P.; Nocera, D. G. *J. Am. Chem. Soc.* **1995**, *117*, 8051−8052. (b) Kirby, J. P.; van Dantzig, N. A.; Change, C. K.; Nocera, D. G. *Tetrahedron Lett.* **1995**, *36*, 3477−3480. (c) Deng, Y.; Roberts, J. A. Peng, S.-M.; Chang, C. K.; Nocera, D. G. *Angew. Chem., Int. Ed. Engl.* **1997**, *36*, 2124−2127. (d) Kirby, J. P.; Roberts, J. A.; Nocera, D. G. *J. Am. Chem. Soc.* **1997**, *119*, 9230−9236.

(7) Nappa, M.; Valentine, J. S. *J. Am. Chem. Soc.* **1978**, *100*, 5075−5080.

(8) (a) Long, J. R.; Drago, R. S. *J. Chem. Educ.* **1982**, *59*, 1037−1039. (b) Horman, I.; Dreux, B. *Helv. Chim. Acta* **1984**, *67*, 754−764.

(9) (a) Miller, J. R.; Dorough, G. D. *J. Am. Chem. Soc.* **1952**, *74*, 3977−3981. (b) Kadish, K. M.; Shiue, L. R.; Rhodes, R. K.; Bottomley, L. A. *Inorg. Chem.* **1981**, *20*, 1274−1277.

(10) (a) Abraham, R. J.; Fell, S. C. M.; Smith, K. M. *Org. Magn. Reson.* **1977**, *9*, 367−373. (b) Abraham, R. J.; Bedford, G. R.; McNeillie, D.; Wright, B. *Org. Magn. Reson.* **1980**, *14*, 418−425. (c) Chachaty, C.; Gust, D.; Moore, T. A.; Nemeth, G. A.; Liddell, P. A.; Moore, A. L. *Org. Magn. Reson.* **1984**, *22*, 39−46.

(11) Ninety percent of the total **D1** and **S1** is in the bound state under these conditions, as calculated from the association constant of 8.1×10^3 M^{-1}.

(12) Otsuki, J.; Narutaki, K. *Bull. Chem. Soc. Jpn.* **2004**, *77*, 1537−1544.

(13) Shin, E. J.; Kim, D. *J. Photochem. Photobiol., A.* **2002**, *152*, 25−31.

(14) Sen, A.; Krishnan, V. *J. Chem. Soc., Faraday Trans.* **1997**, *93*, 4281−4288.

(15) Furhop, J.-H.; Kadish, K. M.; Davis, D. G. *J. Am. Chem. Soc.* **1973**, *95*, 5140−5147.

(16) Connelly, N. G.; Geiger, W. E. *Chem. Rev.* **1996**, *96*, 877−910.

(17) Kadish, K. M.; Shiue, L. R.; Rhodes, R. K.; Bottomley, L. A. *Inorg. Chem.* **1981**, *20*, 1274−1277.

(18) D'Souza, F.; Smith, P. M.; Zandler, M. E.; McCarty, A. L.; Itou, M.; Araki, Y.; Ito, O. *J. Am. Chem. Soc.* **2004**, *126*, 7898−7907.

(19) (a) Kobuke, Y.; Ogawa, K. *Bull. Chem. Soc. Jpn.* **2003**, *76*, 689−708. (b) Ozeki, H.; Nomoto, A.; Ogawa, K.; Kobuke, Y.; Murakami, M.; Hosoda, K.; Ohtani, M.; Nakashima, S.; Miyasaka, H.; Okada, T. *Chem. Eur. J.* **2004**, *10*, 6393−6401.

(20) Wiederrecht, G. P.; Niemczyk, M. P.; Svec, W. A.; Wasielewski, M. R. *J. Am. Chem. Soc.* **1996**, *118*, 81−88.

(21) (a) Osuka, A.; Nakajima, S.; Maruyama, K.; Mataga, N.; Asahi, T. *Chem. Lett.* **1991**, 1003−1006. (b) Osuka, A.; Yamazaki, I.; Nishimura, Y.; Ohno, T.; Nozaki, K. *J. Am. Chem. Soc.* **1996**, *118*, 155−168.

(22) (a) Otsuki, J.; Suka, A.; Yamazaki, K.; Abe, H.; Araki, Y.; Ito, O. *Chem. Commun.* **2004**, 1290−1291. (b) Otsuki, J.; Harada, K.; Toyama, K.; Hirose, Y.; Araki, K.; Seno, M.; Takatera, K.; Watanabe, T. *Chem. Commun.* **1998**, 1515−1516.

(23) The missing columns for **D3S2A1** and **D5S2A1** are due to their different spectral changes not showing axial coordination. The ratio of complexed porphyrin for **D5A1** is simply zero.

(24) Buchler, J. W.; Decian, A.; Fischer, J.; Kruppa, S. B.; Weiss, R. *Chem. Ber.* **1990**, *123*, 2247−2253.

(25) Lin, C.-L.; Fang, M.-Y.; Cheng, S.-H. *J. Electroanal. Chem.* **2002**, *531*, 155−162.

(26) Kashiwagi, Y.; Imahori, H.; Araki, Y.; Ito, O.; Yamada, K.; Sakata, Y.; Fukuzumi, S. *J. Phys. Chem. A* **2002**, *107*, 5515−5522.

(27) Wagner, R. W.; Seth, J.; Yang, S. I.; Kim, D.; Bocian, D. F.; Holten, D.; Lindsey, J. S. *J. Org. Chem.* **1998**, *63*, 5042−5049.

(28) Gregg, B. A.; Cormier, R. A. *J. Am. Chem. Soc.* **2001**, *123*, 7959−7960.

(29) Hatzidimitriou, A.; Gourdon, A.; Devillers, J.; Launay, J.-P.; Meta, E.; Amouyal, E. *Inorg. Chem.* **1996**, *35*, 2212−2219.